Eur Radiol
DOI 10.1007/s00330-017-4820-1

MAGNETIC RESONANCE

Identifying the white matter impairments among ART-naïve HIV patients: a multivariate pattern analysis of DTI data

Zhenchao Tang[1,2] · Zhenyu Liu[2] · Ruili Li[3] · Xin Yang[2] · Xingwei Cui[4] · Shuo Wang[2] · Dongdong Yu[2] · Hongjun Li[3] · Enqing Dong[1] · Jie Tian[2,5]

Received: 14 January 2017 / Revised: 4 March 2017 / Accepted: 17 March 2017

Abstract

Objective To identify the white matter (WM) impairments of the antiretroviral therapy (ART)-naïve HIV patients by conducting a multivariate pattern analysis (MVPA) of Diffusion Tensor Imaging (DTI) data

Methods We enrolled 33 ART-naïve HIV patients and 32 Normal controls in the current study. Firstly, the DTI metrics in whole brain WM tracts were extracted for each subject and feed into the Least Absolute Shrinkage and Selection Operators procedure (LASSO)-Logistic regression model to identify the impaired WM tracts. Then, Support Vector Machines (SVM) model was constructed based on the DTI metrics in the impaired WM tracts to make HIV-control group classification. Pearson correlations between the WM impairments and HIV clinical statics were also investigated.

Results Extensive HIV-related impairments were observed in the WM tracts associated with motor function, the corpus callosum (CC) and the frontal WM. With leave-one-out cross validation, accuracy of 83.08% (P=0.002) and the area under the Receiver Operating Characteristic curve of 0.9110 were obtained in the SVM classification model. The impairments of the CC were significantly correlated with the HIV clinic statics.

Conclusion The MVPA was sensitive to detect the HIV-related WM changes. Our findings indicated that the MVPA had considerable potential in exploring the HIV-related WM impairments.

Key points

- *WM impairments along motor pathway were detected among the ART-naïve HIV patients*
- *Prominent HIV-related WM impairments were observed in CC and frontal WM*
- *The impairments of CC were significantly related to the HIV clinic statics*
- *The CC might be susceptible to immune dysfunction and HIV replication*
- *Multivariate pattern analysis had potential for studying the HIV-related white matter impairments*

Keywords HIV · Diffusion tensor Imaging · White Matter · Multivariate Analysis · Corpus Callosum

Zhenchao Tang, Zhenyu Liu and Ruili Li contributed equally to this article.

Electronic supplementary material The online version of this article (doi:10.1007/s00330-017-4820-1) contains supplementary material, which is available to authorized users.

✉ Hongjun Li
lihongjun00113@126.com

✉ Enqing Dong
enqdong@sdu.edu.cn

✉ Jie Tian
jie.tian@ia.ac.cn

[1] School of Mechanical, Electrical & Information Engineering, Shandong University, Weihai, Shandong Province 264209, China

[2] CAS Key Laboratory of Molecular Imaging, Institute of Automation, Beijing 100190, China

[3] Department of Radiology, Beijing YouAn Hospital, Capital Medical University, Beijing 100069, China

[4] Cooperative Innovation Center of Internet Healthcare, Zhengzhou University, Zhengzhou, China 450052

[5] University of Chinese Academy of Sciences, Beijing 100049, China

Abbreviations

ART	Antiretroviral Therapy
MVPA	Multivariate Pattern Analysis
DTI	Diffusion tensor Imaging

Published online: 10 April 2017

WM	White Matter
FA	Fractional Anisotropy
MD	Mean Diffusivity
AD	Axial Diffusivity
RD	Radial Diffusivity
ROI	Regions of Interests
LASSO	The Least Absolute Shrinkage and Selection Operators procedure
SVM	Support Vector Machines
ACC	Accuracy
ROC	Receiver Operating Characteristic
AUC	Area under the ROC curve
LOOCV	Leave one out cross-validation
CC	Corpus Callosum

Introduction

HIV infection affects the brain soon after seroconversion, bringing about neurodegeneration and subsequently resulting in cognitive impairments [1]. Though the introduction of antiretroviral therapy (ART) has prevented the death from HIV, the therapy has been insufficient to eradicate the neurodegeneration caused by HIV infection [2]. With the advance of the disease, the neurodegeneration of the central nervous system can be exacerbated by the longer exposure to HIV and lead to HIV-associated neurocognitive impairments [3]. Meanwhile, the underlying neuropathological changes of these clinical symptoms are still not completely understood [4, 5]. In recent years, the non-invasive MRI techniques, including T1-weighted MRI, functional MRI (fMRI) and diffusion tensor Imaging (DTI), have shown great effectiveness in studying the HIV-related neurodegeneration [6].

DTI has been an effective tool for detecting the subtle white matter (WM) microstructure changes in HIV infection by measuring the in vivo water molecule diffusion within the WM fibers [7]. WM changes were revealed by the alterations of the DTI deprived metrics, including Fractional Anisotropy (FA), Mean Diffusivity (MD), Axial Diffusivity (AD) and Radial Diffusivity (RD) [8]. Most of the previous DTI studies employed the conventional univariate statistical analysis of the DTI metrics to identify the WM changes due to HIV infection. In the earlier studies, it was found that HIV infection would cause damage to the callosal [9, 10] and frontal [11, 12] WM by investigating the DTI metrics changes in the regions of interests (ROI) [9, 12] and particular WM tracts [10, 11]. While in recent DTI studies employing whole brain voxel-wise analysis and tract-based spatial statistics analysis, HIV infection was found to cause damage in more extensive and variable WM structures, including the corpus callosum (CC) [13–15], the corona radiate [13], the uncinated fasciculus [16], the internal capsule [13, 15], the cerebellar peduncles [17], the cerebral peduncle [15], corticospinal tracts [18], and so on. It was regrettable that discrepancies existed in the findings of the previous univariate statistical analysis studies [6, 19].

In recent years, the multivariate pattern analysis (MVPA) has been increasingly used in DTI researches [20–24]. This method uses the DTI metrics as features to estimate the clinic variables or predict the diagnosis status, and in turn reveal the disease-related DTI metrics changes. The MVPA took inter-regional correlations into account and provided increased sensitivity in detecting the subtle neuropathology changes, which might help to settle the issues in previous univariate statistical analysis studies of HIV, while there had been only a small number of researches applying the MVPA in HIV infection. In a previous study employing the linear mixed-effects model, it was found that HIV disease severity was associated with the disrupted DTI metrics in the inferior fronto-occipital, the uncinate tracts, and the inferior longitudinal fasciculus [25]. In another study, Nir et al. ran a voxel-wise linear regression to test for the effects of HIV diagnosis on WM integrity, and observed widespread WM impairments agreeing with the findings of prior univariate statistical analysis studies [26]. The results of these pioneering studies indicated the potential of the MVPA in studying the HIV-related WM impairments.

Nevertheless, the WM characteristics usually generated a great number of features, which made it difficult to identify the DTI metrics changes crucial for HIV infection [25, 26]. There was an urgent need to select the meaningful and informative features before feeding them into the models. The Least Absolute Shrinkage and Selection Operators procedure (LASSO) regression was capable of selecting the features associated with the dependence variable and forcing the coefficients of irrelevant features towards zeros, which offered a possible solution to this problem [27]. In a previous study employing LASSO regression on several limited brain regions, Bunea et al. found that the DTI metrics changes in the CC and internal capsule were related to the neurocognitive dysfunction among HIV patients [28], which indicated that the LASSO regression was suitable to detect the HIV-related WM changes.

In the current study, we aimed to employ the LASSO regression to identify the WM tracts impairments associated with HIV infection. Particularly, the analysis of the current study was confined to the ART naïve patients to exclude the possible factor of ART erosion on the WM integrity [29]. To further ascertain that the identified tracts were truly related to HIV infection, a Support Vector Machines (SVM) model based on the selected features was constructed to make the HIV-control classification. The SVM is an algorithm designed for binary classification that maximizes the margins between classes in a high dimensional space, and was well-suited to distinguish the individuals with WM degeneration disease [22, 30, 31]. The SVM classification model would be assessed by classification accuracy (ACC) and the area under the Receiver Operating Characteristic (ROC) curve (AUC).

Relatively high ACC and AUC values would further confirm that the WM impairments identified by the LASSO regression were substantially associated with HIV infection.

Materials and methods

Subjects and data acquisition

The study was approved by the Ethics Committee of the Beijing YouAn Hospital, Capital Medical University. 33 HIV patients and 32 age and gender-matched normal control (NC) subjects were employed in the current study. All the subjects had provided written informed consent after a detailed explanation of this study. The HIV patients were enrolled from the Beijing YouAn Hospital, Capital Medical University. All the HIV patients were naïve to ART. The exclusion criterion for HIV patients included: history of alcohol or substance abuse, obvious brain lesion (such as trauma or tumours), history of neurodegenerative disease other than HIV (such as diabetes, and Alzheimer's disease), diagnosis of neurological comorbidities (such as HIV encephalitis or leukoencephalopathy). The clinical statics, including current $CD4^+$ cell counts, $CD4^+/CD8^+$ ratios, and plasma viral loads were collected for each patient. The duration of HIV infection was determined by self-reports of patients. The NC subjects were enrolled from the same urban areas as the infected subjects. The NC subjects were confirmed to be exclusive of obvious brain lesion (such as trauma or tumours), any history of previous neurodegenerative disease (such as diabetes, and Alzheimer's disease) or systemic disease. The demographic and clinical information of HIV patients and NC subjects is provided in Table 1.

For each subject, structural T1-weighted MRI and DTI were obtained on a 3.0T Siemens scanner (Allegra, Siemens Medical System, Erlangen, Germany) using a 32-channel phased array coil. A standard birdcage head coil and restraining foam pads were used to minimize head motion. Structural T1-weighted MRI was acquired with a spoiled gradient recall sequence. For DTI, we used single shot echo-planar imaging (EPI) sequences in contiguous axial planes covering the whole brain. Detailed acquisition parameters are listed in Table 2. All the MRI were reviewed by an experienced neuroradiologist and confirmed exclusive of visible brain damages.

Whole brain WM characteristics

We employed the ROI-based analysis to investigate the whole brain white matter characteristics. The ROI-based analysis was performed based on the International Consortium for Brain Mapping DTI-81 (ICBM DTI-81) WM labels atlas [32], which identified 50 main WM tracts in the Montreal Neurological Institute (MNI) 152 space. The FMRIB Software Library (FSL, FMRIB, Oxford, UK) [33–35] and a Pipeline for analyzing brain diffusion images (PANDA) [36] (http://www.nitrc.org/projects/panda) were employed for DTI data processing. Firstly, the maps of FA, MD, AD and RD were obtained by DTI preprocessing in a similar procedure with the previous DTI studies [37–40]. Then, the FA, MD, AD and RD maps in the native space were non-linearly registered to the FMRI58-FA template (http://fsl.fmrib.ox.ac.uk/fsl/fslwiki/FMRIB58_FA) in the MNI 152 space. Subsequently, the mean FA, MD, AD, and RD values in each WM tract were calculated for each subject. The 200 DTI metrics of FA, MD, AD, and RD values representing the whole brain WM characteristics were used as features in the following process.

Feature selection

In the current study, the feature selection was realized using the LASSO-Logistic regression model implemented within the Glmnet [41] (http://statweb.stanford.edu/~tibs/lasso.html). The LASSO regression selected the features most related to HIV infection by shrinking the coefficients of unrelated features towards zero with the regulation parameter λ. The regulation parameter λ tuned the sparsity of the model: a larger λ would lead to a sparser model. By choosing appropriate λ, the LASSO regression reduced the chance of model overfitting, and simultaneously achieved the goodness of model fitting. We chose the regulation parameter λ with the cyclical coordinate descent method, where the minimal λ was set as 0.1; and the number of λ was set as 100. We obtained the mean misclassification rate for each λ with the leave-one-out cross-validation (LOOCV) method. The λ obtaining the minimum mean misclassification rate in the LASSO-Logistic regression model was chosen as the optimal regulation parameter. The features in the model with optimal regulation parameters were regarded as selected features.

The selected features represented the HIV-related DTI metrics alterations, revealing the microstructure degenerations in different WM tracts. To investigate the statistical significance of the DTI measures changes, two sample T tests were conducted on all the selected features between the HIV group and the NC group with SPSS18 (http://www.ibm.com/analytics/us/en/technology/spss/). Significance was set as $P<0.05$.

HIV-control group classification

Based on the features selected by LASSO regression analysis, we employed the SVM with linear kernel to construct the HIV-control group classification model. Due to the limited sample size in the current study, we employed the LOOCV strategy to assess the classification

Table 1 Demographic and clinical information of the subjects enrolled in the current study

Items	HIV patients	NC subjects	*P*-value
Age (Year)	31.12±6.39	31.81±7.42	0.688
Gender (Male/Female)	24/9	17/15	0.102
Current $CD4^+$ cell counts (Cell/μL)	256.86±198.57	-	-
$CD4^+/CD8^+$ ratios	0.52±1.37	-	-
Plasma viral loads (log_{10} copies/mL)	4.34±1.03	-	-
Disease duration (Months)	25.18±18.23	-	-

Data are presented as mean ± standard deviation. *P*-values are calculated by independent-samples T test for age and Chi-square test for Sex

performance of the SVM model. Based on the results of LOOCV, we plotted the ROC curve, and calculated the AUC and the classification ACC. In addition, we also obtained the weight value of each feature in constituting the hyperplane of the SVM model. The weight value of each feature was calculated by summing the weight coefficients assigned to the feature across the 65 LOOCV loop, and subsequently dividing the maximal coefficients across all the selected features. The SVM parameters were set to acquire the best classification performance.

A permutation test was conducted to assess the statistical significance of the ACC obtained by the SVM model with a framework implemented in previous studies [42–44]. Firstly, the label of each subject was randomly permutated for 500 times and assigned to all the subjects. Then, the SVM classification model was reconstructed based on the permutated labels to obtain the permutated ACCs. The *P*-value was defined as below, indicating how likely the classification performance of the SVM model was observed by chance:

$$P = \frac{1 + N_{greater\,ACC}}{1 + N} \quad (1)$$

where N was the number of permutations, which was 500 here; $N_{\text{greater ACC}}$ was the number of the permutations which obtained greater ACC than the non-permutation ACC. The classification ACC of the SVM model was considered as statistical significant on the condition that the non-permutated ACC was greater than 95% of the permutated ACC, corresponding to $P < 0.05$.

Correlation analysis

To investigate the association between the HIV-related WM changes and the clinical statistics, we carried out Pearson correlations analysis of the selected features with the current $CD4^+$ cell counts, plasma viral loads, and $CD4^+/CD8^+$ ratios. The plasma viral loads were not normally distributed, and were log transformed (10 based) prior to statistical analysis. The correlation analysis was conducted within the patient groups. Pearson correlation analysis was conducted with SPSS18. Significance was set as $P<0.05$. The *P* values were Bonferroni-corrected for the number of the clinical statistics (the current $CD4^+$ cell counts, plasma viral loads, and $CD4^+/CD8^+$ ratios).

Table 2 Acquisition parameters for Structural T1-weighted MRI and DTI

Scan parameters (TI/TR/TE)	Structural T1-weighted MRI 900ms/1900ms/2.52ms	DTI -/3300ms/90ms
Field of view	250 × 250mm	230 × 230mm
Acquisition matrix	256 × 246	128 × 128
Number of slices	176	25
Slice thickness	1mm	4mm
Flip angle	9°	90°
Scan time	4 min 18s	3 min 39s
Non-collinear Directions	-	20
Max b-value	-	1000 s/mm^2
Number of b0 volume	-	3

TI Inversion time; *TR* Repetition Time; *TE* Echo Time

Table 3 The impaired WM tracts identified in LASSO regression analysis

	Impaired WM tracts	Group Differences between HIV and NC		Weight values
		t value	*P* value	
FA	CP.R	-1565	0.123	0.578
	CP.L	-2.254	0.028*	0.147
	ALIC.R	1.412	0.163	1.000
	ACR.R	0.570	0.571	0.686
	TAP.R	-2.237	0.029*	0.499
MD	GCC	4.481	<0.001*	0.237
	ICP.R	2.318	0.024*	0.366
	PLIC.L	-1.190	0.239	0.724
	FX/ST.L	3.376	0.001**	0.287
AD	GCC	4.665	<0.001*	0.426
	BCC	3.698	<0.001*	0.484
	ACR.R	3.393	0.001*	0.250
	SS.L	3.580	0.001*	0.683
	SFO.L	2.702	0.009*	0.643
	UNC.R	3.126	0.003*	0.525
	TAP.R	0.224	0.823	0.466
RD	CST.R	1.415	0.162	0.604
	FX/ST.L	3.208	0.002*	0.447

The abbreviations of the tracts are: *GCC* Genu of Corpus callosum; *BCC* Body of Corpus callosum; *CST* Corticospinal tracts; *ICP* Inferior cerebellar peduncle; *CP* Cerebral peduncle; *ALIC* Anterior limb of internal capsule; *PLIC* Posterior limb of internal capsule; *ACR* Anterior corona radiate; *SS* Sagittal stratum; *FX/ST* Fornix and stria terminalis; *SFO* Superior fronto-occipital fasciculus; *UNC* Uncinate fasciculus; *TAP* Tapetum. *R, L* represented right and left lateral, respectively. * indicated $P<0.05$. The weighted values were obtained from the weight coefficients of each feature in constituting the hyperplane of the SVM model

Results

WM impairments among ART naïve HIV patients

Eighteen features associated with HIV infection were selected by LASSO regression analysis, indicating that HIV-infection brought about DTI metrics changes in the selected WM tracts (Table 3). As shown in Table 3, HIV-infection led to alterations in all the four DTI metrics of FA, MD, AD and RD. WM impairments were found in the tracts crucial to motor function, including the corticospinal tracts, the inferior cerebellar peduncle, the cerebral peduncle, and the posterior limb of the internal capsule. Specially, the WM along the descending motor pathway on the left lateral (the left posterior limb of

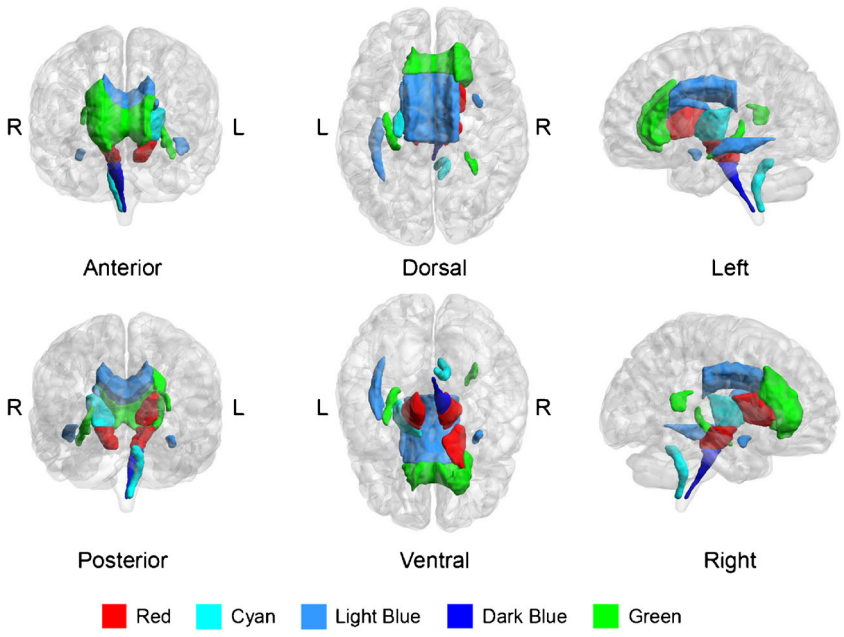

Fig. 1 The impaired WM tracts identified in LASSO regression analysis (Red represents the tracts of FA changes; Cyan represents the tracts of MD changes; Light Blue represents the tracts of AD changes; Dark Blue represents the tracts of RD changes; Green represents the tracts of multi DTI metrics changes)

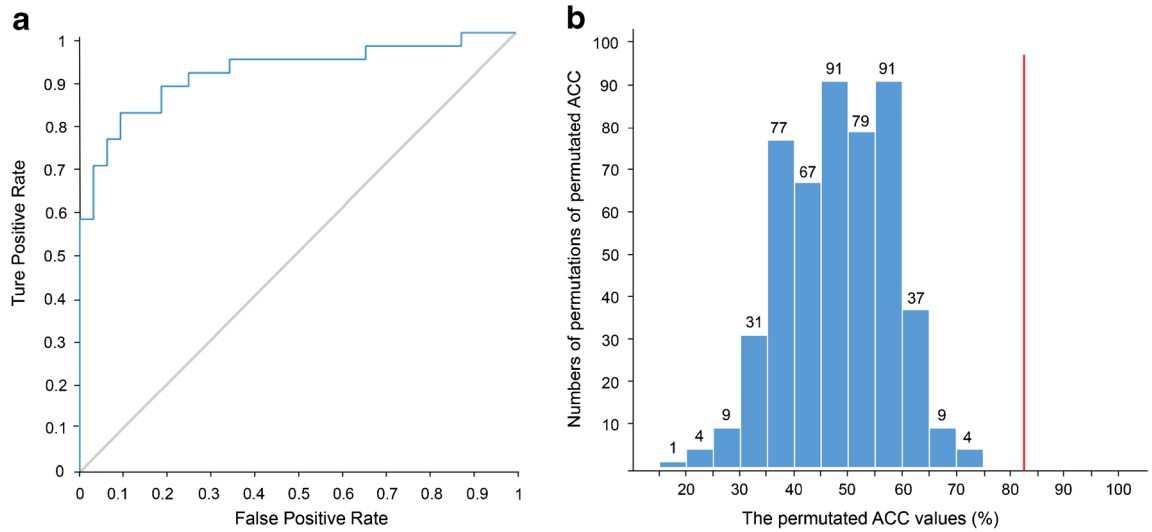

Fig. 2 **a**) The ROC curve of the HIV-Control group classification model based on leave-one-out cross-validation, AUC=0.9110; **b**) the distribution of the permutated ACC values. The red line indicates the non-permutation ACC value (83.08%). Each bar represents the number of permutations which obtained the ACC within the corresponding range. As can be seen from the illustration, no better classification ACC was observed in the 500 permutations

the internal capsule, the left cerebral peduncle, and the right corticospinal tracts) was involved in HIV infection. Apart from the WM tracts associated with motor function, most of the WM impairments were observed in the CC and the frontal WM. The 3-D views of the impaired WM tracts in HIV infection are illustrated in Fig. 1. The illustration of the λ obtaining the minimum mean misclassification rate and the coefficients of the selected features are provided in the Electronic Supplementary Material (Fig.S1 and Fig.S2).

In the group difference analysis of selected features, 12 out of the 18 features were found significantly different between the HIV group and NC group (Table 3). In comparison with the NC group, a pattern of increased FA values, and decreased MD, AD, RD values were observed in the HIV group.

HIV-control group classification results

Based on the features selected by the LASSO regression analysis, AUC of 0.9110 and ACC of 83.08% were achieved by the SVM classification model with LOOCV strategy. The ROC curve of the classification model was plotted (as showed in Fig. 2a). The ACC was confirmed to be statistically significant (P=0.002) as no superior ACC was observed in the 500 permutations (Fig. 2b). The weight values of the selected features in the SVM model are provided in Table 3.

Correlation analysis results

After Bonferroni-correction, the increased MD values in the genu of CC were found significantly correlated with the lower current $CD4^+$ cell counts (r= -0.495; P=0.009), the lower $CD4^+/CD8^+$ ratios (r= -0.462; P=0.021), and the higher plasma viral loads (r= 0.418; P= 0.048). The increased AD values in the genu of the CC were significantly correlated with the lower current $CD4^+$ cell counts (r= -0.454; P=0.024) after correction. The scatter diagrams are illustrated in Fig. 3.

Discussion

In the current study, we employed the MVPA method on DTI data to investigate the impaired WM tracts among the ART naïve HIV patients. LASSO regression analysis was employed to select the DTI metrics associated with HIV diagnosis status, revealing the impaired WM tracts in HIV infection. We found widespread impairments in the motor function-related WM tracts, the CC and the frontal WM. The DTI measures in the impaired WM tracts were also found effective to distinguish the HIV patients from NC individuals, as indicated in the SVM analysis.

We found that HIV infection would lead to WM impairments in the tracts crucial to motor function. Especially, the WM impairments were observed in the left posterior limb of the internal capsule, the left cerebral peduncle, and the right corticospinal tracts, which rightly constituted the descending motor pathway. The descending motor pathway was responsible for conveying the motor commands from the precentral gyrus to the lower motor neurons in order to conduct muscular movements. Our results of WM impairments on the descending motor pathway agreed with the findings in previous studies which reported that the motor impairments were highly prevalent among HIV-infected patients, especially among the

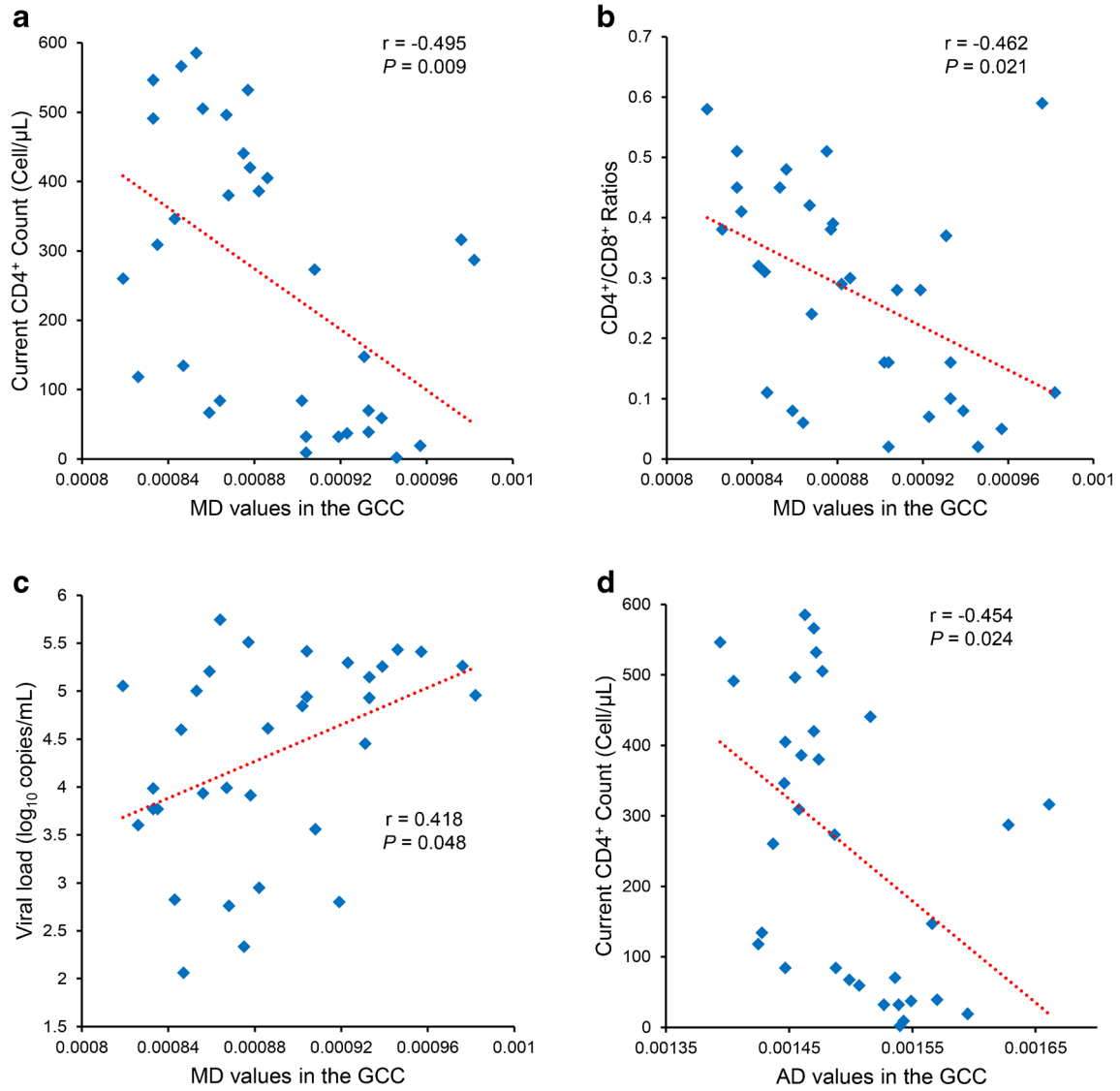

Fig. 3 The WM impairments in the genu of CC were significantly correlated with the HIV clinical characteristics. a) The increased MD values in the genu of CC were negatively correlated with the current $CD4^+$ counts; b) The increased MD values in the genu of CC were negatively correlated with the $CD4^+/CD8^+$ ratios; c) The increased MD values in the genu of CC were positively correlated with the viral load; d) The increased AD values in the genu of CC were negatively correlated with the current $CD4^+$ counts. GCC, genu of corpus callosum. The *P* values were Bonferroni-corrected for the number of the clinical statistics

individuals naïve to ART [45–47]. It was interesting to note that WM impairments in the internal capsule [13, 48, 49], the cerebral peduncle [15, 26] and the corticospinal tracts [18, 50] had been respectively observed in previous univariate analysis studies. However, it had not been reported that the three tracts were simultaneously involved in HIV infection. We supposed this might be due to the MVPA being sensitive to the subtle neuropathology changes, thus detection of the WM integrity changes were not observed in previous studies.

Apart from the tracts associated with motor function, most of the observed WM impairments were located in the CC and frontal lobe. Our findings of HIV-related WM impairments in the genu and body of CC [14, 51–53], the anterior corona radiate [13, 15, 54], the anterior limb of internal capsule [26, 48], the superior fronto-occipital fasciculus [49, 55], and the uncinate fasciculus [16, 17, 25] agreed with the results of previous univariate statistical analysis studies of HIV. Though we also found impaired white matter tracts distant from the frontal lobe (the fornix and stria terminalis, sagittal stratum and tapetum), it can be observed that most of the impaired white matter tracts exhibited a pattern of centering on the frontal lobe. It might be inferred that the frontal WM was especially vulnerable to HIV infection.

In the correlation analysis, we found that the increased MD values in the genu of CC were significantly correlated to the lower current $CD4^+$ cell counts, the

lower $CD4^+$:$CD8^+$ ratios and the higher plasma viral loads. Clinically, the lower current $CD4^+$ cell counts indicated the immune suppression in HIV infection [56], and the lower $CD4^+$:$CD8^+$ ratios implied immunosenescence [57]. The higher plasma viral loads represented the HIV activity and replication in the body's internal environment. Our result might indicate that the WM microstructure in the genu of CC was susceptible to the immune dysfunction and viral replication in HIV infection. We also found that the increased AD values in the genu of CC were significantly correlated to the lower current $CD4^+$ cell counts. As indicated in previous study, the abnormalities of AD values were related to axonal injury [58]. It might imply that the immune suppression emerged among the ART naïve HIV patients would accelerate the axonal injury in the genu of CC.

In the SVM model based on the DTI metrics in the impaired WM tracts, we achieved AUC of 0.9110 and ACC of 83.08% in making the HIV control group classification. Furthermore, no better classification ACC was observed than the non-permutated ACC in the permutation test. The results further confirmed that the impaired WM tracts identified in LASSO regression analysis were substantially associated with HIV infection.

The current study has several limitations. First, the sample size of the study was relatively small. Sixty-five subjects might be an adequate sample for a neuroimaging study, but it is a small sample for the construction of a HIV-control classification model. Though we employed cross-validation in the current study to settle the issue, it will be still important to verify the classification results by independent validation with a larger sample size cohort. Secondly, the data of the current study was cross-sectional, which limited us from exploring the longitudinal WM changes due to HIV infection. Future longitudinal study with a larger sample size will still be needed to provide deeper insight into the WM degenerations in HIV infection.

In conclusion, we found widespread WM impairments among the ART naïve HIV patients by employing the MVPA method on DTI data. The MVPA method was sensitive to subtle WM changes, and detected the compromise of the WM along the motor pathway in HIV infection. With the MVPA of DTI data, prominent WM impairments agreeing with the previous studies were observed in the CC and frontal WM. Our findings implied that the MVPA had considerable potential in exploring the HIV-related WM changes.

Acknowledgements This paper was supported by the National Natural Science Foundation of China under Grant No. 81671848, 81501549, 81527805, 81371635, 81227901, 61231004, 81571634, the Science and Technology Service Network Initiative Program of Chinese Academy of Science under Grant NO. KFJ-SW-STS-160, the Strategic Priority Research Program from the Chinese Academy of Sciences under Grant NO. XDB02060010, the Beijing Municipal Science & Technology Commission No. Z161100002616022, the Beijing Municipal Administration of Hospitals Clinical Medicine Development of Special Funding under Grant NO. ZYLX201511, and the Beijing Municipal Administration of Hospitals Incubating Program under Grant NO. PX2016036. The study was approved by the Ethics Committee of the Beijing YouAn Hospital, Capital Medical University. All the subjects had provided written informed consent after a detailed explanation of this study. The authors would like to express their deep appreciation to all anonymous reviewers for their kind comments.

Compliance with ethical standards

Guarantor The scientific guarantor of this publication is Jie Tian.

Conflict of interest The authors of this manuscript declare no relationships with any companies, whose products or services may be related to the subject matter of the article.

Funding This paper is supported by the National Natural Science Foundation of China under Grant No. 81671848, 81501549, 81527805, 81371635, 81227901, 61231004, 81571634, Science and Technology Service Network Initiative Program of Chinese Academy of Science under Grant NO. KFJ-SW-STS-160, the Strategic Priority Research Program from Chinese Academy of Sciences under Grant NO. XDB02060010, the Beijing Municipal Science & Technology Commission No. Z161100002616022, the Beijing Municipal Administration of Hospitals Clinical Medicine Development of Special Funding under Grant NO. ZYLX201511, and the Beijing Municipal Administration of Hospitals Incubating Program under Grant NO. PX2016036.

Statistics and biometry No complex statistical methods were necessary for this paper.

Informed consent Written informed consent was obtained from all subjects (patients) in this study.

Ethical approval The study was approved by the Ethics Committee of the Beijing YouAn Hospital, Capital Medical University.

Methodology
- retrospective
- cross sectional study
- performed at one institution

References

1. Ellis R, Langford D, Masliah E (2007) HIV and antiretroviral therapy in the brain: neuronal injury and repair. Nat Rev Neurosci 8:33–44
2. Vassallo M, Durant J, Biscay V et al (2014) Can high central nervous system penetrating antiretroviral regimens protect against the onset of HIV-associated neurocognitive disorders? Aids 28:493–501
3. Ances BM, Hammoud DA (2014) Neuroimaging of HIV-associated neurocognitive disorders (HAND). Curr Opin HIV AIDS 9:545–551
4. Clifford DB, Ances BM (2013) HIV-associated neurocognitive disorder. Lancet Infect Dis 13:976–986

5. Nightingale S, Winston A, Letendre S et al (2014) Controversies in HIV-associated neurocognitive disorders. Lancet Neurol 13:1139–1151
6. Thompson PM, Jahanshad N (2015) Novel Neuroimaging Methods to Understand How HIV Affects the Brain. Curr HIV/AIDS Rep 12: 289–298
7. Rahimian P, He JJ (2016) HIV/neuroAIDS biomarkers. Prog Neurobiol. doi:10.1016/j.pneurobio.2016.04.003
8. Basser PJ, Mattiello J, LeBihan D (1994) MR diffusion tensor spectroscopy and imaging. Biophys J 66:259–267
9. Wright PW, Heaps JM, Shimony JS, Thomas JB, Ances BM (2012) The effects of HIV and combination antiretroviral therapy on white matter integrity. Aids 26:1501–1508
10. Pfefferbaum A, Rosenbloom MJ, Adalsteinsson E, Sullivan EV (2007) Diffusion tensor imaging with quantitative fibre tracking in HIV infection and alcoholism comorbidity: synergistic white matter damage. Brain 130:48–64
11. Pfefferbaum A, Rosenbloom MJ, Rohlfing T, Kemper CA, Deresinski S, Sullivan EV (2009) Frontostriatal fiber bundle compromise in HIV infection without dementia. Aids 23:1977–1985
12. Chen Y, An H, Zhu H et al (2009) White matter abnormalities revealed by diffusion tensor imaging in non-demented and demented HIV+ patients. Neuroimage 47:1154–1162
13. Wang B, Liu Z, Liu J, Tang Z, Li H, Tian J (2016) Gray and white matter alterations in early HIV-infected patients: Combined voxel-based morphometry and tract-based spatial statistics. J Magn Reson Imaging 43:1474–1483
14. Wright PW, Vaida FF, Fernandez RJ et al (2015) Cerebral white matter integrity during primary HIV infection. Aids 29:433–442
15. Hoare J, Fouche JP, Phillips N et al (2015) White matter microstructural changes in ART-naive and ART-treated children and adolescents infected with HIV in South Africa. Aids 29:1793–1801
16. Correa DG, Zimmermann N, Doring TM et al (2015) Diffusion tensor MR imaging of white matter integrity in HIV-positive patients with planning deficit. Neuroradiology 57:475–482
17. Tran LT, Roos A, Fouche JP et al (2016) White Matter Microstructural Integrity and Neurobehavioral Outcome of HIV-Exposed Uninfected Neonates. Medicine (Baltimore) 95, e2577
18. Ackermann C, Andronikou S, Saleh M et al (2016) Early Antiretroviral Therapy in HIV-Infected Children Is Associated with Diffuse White Matter Structural Abnormality and Corpus Callosum Sparing. Am J Neuroradiol
19. Masters MC, Ances BM (2014) Role of neuroimaging in HIV-associated neurocognitive disorders. Semin Neurol 34:89–102
20. Hu X, Liu Q, Li B et al (2016) Multivariate pattern analysis of obsessive–compulsive disorder using structural neuroanatomy. Eur Neuropsychopharmacol 26:246–254
21. Bertocci MA, Bebko G, Versace A et al (2016) Predicting clinical outcome from reward circuitry function and white matter structure in behaviorally and emotionally dysregulated youth. Mol Psychiatry 21:1194–1201
22. Li F, Huang X, Tang W et al (2014) Multivariate pattern analysis of DTI reveals differential white matter in individuals with obsessive-compulsive disorder. Hum Brain Mapp 35:2643–2651
23. Bron EE, Smits M, Papma JM et al (2016) Multiparametric computer-aided differential diagnosis of Alzheimer's disease and frontotemporal dementia using structural and advanced MRI. Eur Radiol. doi:10.1007/s00330-016-4691-x
24. Kamagata K, Hatano T, Okuzumi A et al (2016) Neurite orientation dispersion and density imaging in the substantia nigra in idiopathic Parkinson disease. Eur Radiol 26:2567–2577
25. Uban KA, Herting MM, Williams PL et al (2015) White matter microstructure among youth with perinatally acquired HIV is associated with disease severity. Aids 29:1035–1044
26. Nir TM, Jahanshad N, Busovaca E et al (2014) Mapping white matter integrity in elderly people with HIV. Hum Brain Mapp 35: 975–992
27. Tibshirani R (1996) Regression shrinkage and selection via the Lasso. J R Stat Soc Ser B Methodol 58:267–288
28. Bunea F, She Y, Ombao H, Gongvatana A, Devlin K, Cohen R (2011) Penalized least squares regression methods and applications to neuroimaging. Neuroimage 55:1519–1527
29. Shah A, Gangwani MR, Chaudhari NS, Glazyrin A, Bhat HK, Kumar A (2016) Neurotoxicity in the Post-HAART Era: Caution for the Antiretroviral Therapeutics. Neurotox Res 30:677–697
30. Fang P, An J, Zeng LL et al (2015) Multivariate pattern analysis reveals anatomical connectivity differences between the left and right mesial temporal lobe epilepsy. Neuroimage Clin 7:555–561
31. Grana M, Termenon M, Savio A et al (2011) Computer aided diagnosis system for Alzheimer disease using brain diffusion tensor imaging features selected by Pearson's correlation. Neurosci Lett 502:225–229
32. Mori S, Oishi K, Jiang H et al (2008) Stereotaxic white matter atlas based on diffusion tensor imaging in an ICBM template. Neuroimage 40:570–582
33. Smith SM, Jenkinson M, Woolrich MW et al (2004) Advances in functional and structural MR image analysis and implementation as FSL. Neuroimage 23:S208–S219
34. Smith SM (2002) Fast robust automated brain extraction. Hum Brain Mapp 17:143–155
35. Woolrich MW, Jbabdi S, Patenaude B et al (2009) Bayesian analysis of neuroimaging data in FSL. Neuroimage 45:S173–S186
36. Cui Z, Zhong S, Xu P, He Y, Gong G (2013) PANDA: a pipeline toolbox for analyzing brain diffusion images. Front Hum Neurosci 7:42
37. Tang Z, Dong E, Liu J et al (2016) Longitudinal assessment of fractional anisotropy alterations caused by simian immunodeficiency virus infection: a preliminary diffusion tensor imaging study. J Neurovirol 22:231–239
38. Gunbey HP, Bilgici MC, Aslan K et al (2016) Structural brain alterations of Down's syndrome in early childhood evaluation by DTI and volumetric analyses. Eur Radiol. doi:10.1007/s00330-016-4626-6
39. Ryu CW, Park MS, Byun JY, Jahng GH, Park S (2016) White matter integrity associated with clinical symptoms in tinnitus patients: A tract-based spatial statistics study. Eur Radiol 26:2223–2232
40. Wilting J, Rolfsnes HO, Zimmermann H et al (2016) Structural correlates for fatigue in early relapsing remitting multiple sclerosis. Eur Radiol 26:515–523
41. Friedman J, Hastie T, Tibshirani R (2010) Regularization Paths for Generalized Linear Models via Coordinate Descent. J Stat Softw 33:1–22
42. Ojala M, Garriga GC (2010) Permutation Tests for Studying Classifier Performance. J Mach Learn Res 11:1833–1863
43. Tian L, Ma L, Wang L (2016) Alterations of functional connectivities from early to middle adulthood: Clues from multivariate pattern analysis of resting-state fMRI data. Neuroimage 129:389–400
44. Zeng LL, Shen H, Liu L et al (2012) Identifying major depression using whole-brain functional connectivity: a multivariate pattern analysis. Brain 135:1498–1507
45. Bernard C, Dilharreguy B, Allard M et al (2013) Muscular weakness in individuals with HIV associated with a disorganization of the cortico-spinal tract: a multi-modal MRI investigation. Plos One 8, e66810
46. DeVaughn S, Muller-Oehring EM, Markey B, Bronte-Stewart HM, Schulte T (2015) Aging with HIV-1 Infection: Motor Functions, Cognition, and Attention–A Comparison with Parkinson's Disease. Neuropsychol Rev 25:424–438

47. Wilson TW, Heinrichs-Graham E, Robertson KR et al (2013) Functional brain abnormalities during finger-tapping in HIV-infected older adults: a magnetoencephalography study. J Neuroimmune Pharmacol 8:965–974
48. Tang VM, Lang DJ, Giesbrecht CJ et al (2015) White matter deficits assessed by diffusion tensor imaging and cognitive dysfunction in psychostimulant users with comorbid human immunodeficiency virus infection. BMC Res Notes 8:515
49. Zhu T, Zhong J, Hu R et al (2013) Patterns of white matter injury in HIV infection after partial immune reconstitution: a DTI tract-based spatial statistics study. J Neurovirol 19:10–23
50. Stubbe-Drger B, Deppe M, Mohammadi S et al (2012) Early microstructural white matter changes in patients with HIV: a diffusion tensor imaging study. BMC Neurol 12:23
51. Heaps-Woodruff JM, Wright PW, Ances BM, Clifford D, Paul RH (2016) The impact of human immune deficiency virus and hepatitis C coinfection on white matter microstructural integrity. J Neurovirol 22:389–399
52. Kelly SG, Taiwo BO, Wu Y et al (2014) Early suppressive antiretroviral therapy in HIV infection is associated with measurable changes in the corpus callosum. J Neurovirol 20:514–520
53. Leite SC, Correa DG, Doring TM et al (2013) Diffusion tensor MRI evaluation of the corona radiata, cingulate gyri, and corpus callosum in HIV patients. J Magn Reson Imaging 38:1488–1493
54. Kamat R, Brown GG, Bolden K et al (2014) Apathy is associated with white matter abnormalities in anterior, medial brain regions in persons with HIV infection. J Clin Exp Neuropsychol 36:854–866
55. Hoare J, Fouche JP, Phillips N et al (2015) Clinical associations of white matter damage in cART-treated HIV-positive children in South Africa. J Neurovirol 21:120–128
56. Sousa AE, Carneiro J, Meier-Schellersheim M, Grossman Z, Victorino RMM (2002) CD4 T cell depletion is linked directly to immune activation in the pathogenesis of HIV-1 and HIV-2 but only indirectly to the viral load. J Immunol 169:3400–3406
57. Sainz T, Serrano-Villar S, Diaz L et al (2013) The CD4/CD8 ratio as a marker T-cell activation, senescence and activation/exhaustion in treated HIV-infected children and young adults. Aids 27:1513–1516
58. Sun SW, Liang HF, Trinkaus K, Cross AH, Armstrong RC, Song SK (2006) Noninvasive detection of cuprizone induced axonal damage and demyelination in the mouse corpus callosum. Magn Reson Med 55:302–308